Ruthenium Tris(bipyridine)-Centered Linear and Star-Shaped Polystyrenes: Making Atom Transfer Radical Polymerization and Metal Complex Initiators Compatible

Xufeng Wu, James E. Collins, John E. McAlvin, Russell W. Cutts, and Cassandra L. Fraser*

Department of Chemistry, University of Virginia, McCormick Road, P.O. Box 400319, Charlottesville, Virginia 22904-4319

Received October 10, 2000

ABSTRACT: The ligand derivative, 4,4′-bis(chloromethyl)-2,2′-bipyridine (bpy$(CH_2Cl)_2$), and Ru(II) complexes with 2, 4, or 6 pendant halomethyl groups were employed as initiators in the atom transfer radical polymerization (ATRP) of styrene to produce linear and star polymers with ligands and chromophores at discrete positions in the polymer architectures. With the metalloinitiators, [Ru(bpy)$_n$-{bpy$(CH_2Cl)_2$}$_{3-n}$]$(PF_6)_2$ (n = 0, 1, 2), styrene polymerizations were run in bulk monomer, as well as in the presence of small amounts of anisole (14% v/v vs styrene), employing either CuCl/2bpy$(C_{13}H_{27})_2$ or CuBr/1,1,4,7,10,10-hexamethyltriethylenetetraamine (HMTETA) as the ATRP catalyst. Kinetics experiments were performed to determine the level of molecular weight control that is attainable in these polymerizations. With the former catalyst and when anisole is added, reactions exhibited increased control for the metalloinitiators and ligand initiators. Since the dicationic metalloinitiators exhibited limited solubility, which correlated with poor initiation, attempts were made to improve the compatibility of metalloreagents in the nonpolar ATRP medium. Di- and tetrafunctional metalloinitiators modified with alkyl chains, [Ru{bpy$(C_{13}H_{27})_2$}$_n${bpy$(CH_2Cl)_2$}$_{3-n}$]$(PF_6)_2$ (n = 1, 2), displayed improved initiation and molecular weights closer to targeted values. However, attempts to improve the solubility of the homoleptic complex, [Ru{bpy$(CH_2Cl)_2$}$_3$]$(PF_6)_2$ by substituting a $BAr'_4{}^-$ counterion for $PF_6{}^-$ did not enhance molecular weight control. The use of DMF, a more polar solvent, in place of anisole did increase solubility of the hexafunctional initiator; at low monomer conversion, polydispersities were lower in DMF vs anisole. Polymers were characterized by gel permeation chromatography (GPC) with refractive index (RI) and multiangle laser light scattering (MALLS) detection, by UV/vis spectroscopy to confirm the covalent attachment of Ru(II) chromophores to polystyrene chains, and by modulated differential scanning calorimetry (MDSC).

Introduction

Metal-containing polymers have long been of interest for applications in catalysis, as models of biological systems, and for other types of responsive and conducting materials.[1] Both step growth and chain growth mechanisms have been successfully employed in the synthesis of metal-containing polymers using metallomonomers. Often these materials are limited to lower molecular weights due to their poor solubility in many reaction media. In some cases, this issue has been addressed by random copolymerization of metal-containing and metal-free monomers; however, this approach affords little control over the spacing and local environment surrounding the metal center. As is illustrated by metalloproteins and enzymes, greater control over the local environment surrounding a metal center, both its molecular weight and electronic nature, can lead to increased reactivity or uniformity in response to the surrounding environment. And while many applications benefit from high metal loading, the diversity of roles that nature's metal-containing macromolecules play, combined with their efficacy and selectivity, suggests many possible uses for materials with low metal loading.[2]

One way to improve molecular weight and architectural control in macromolecular synthesis is by "living" polymerization.[3] Since termination and chain transfer side reactions are minimal, average molecular weights are determined by reaction stoichiometry; block copolymers, star-shaped polymers, combs, and other elaborate structures have been achieved.[4] Recently, we have explored both metalloinitiation (Figure 1) and macroligand chelation routes to polymeric metal complexes using controlled and living polymerizations.[5] The divergent metalloinitiation route requires compatibility between metal complexes and polymerization reactions. By employing metal bipyridine complexes as initiators in cationic,[6,7] radical,[8,9] and ring-opening[10] reactions, systematic variation of the polymer architecture was achieved through manipulation of the ligand set surrounding the metal template. Polymer composition was modified using different monomers and, for block copolymers, through the order of monomer addition. An alternative approach to polymeric metal complexes

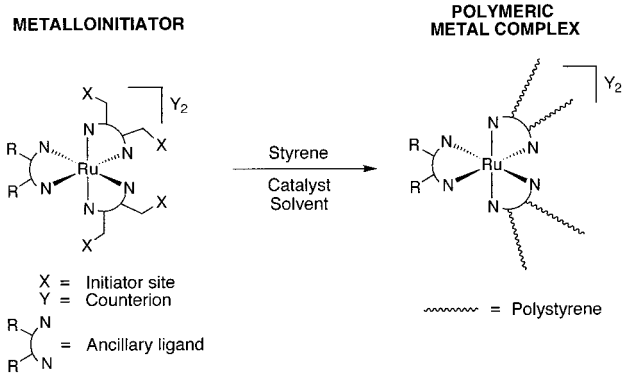

Figure 1. Divergent metalloinitiation approach to polymeric metal complexes. Some reaction parameters that may be varied to optimize molecular weight control in the atom radical polymerization (ATRP) of styrene are indicated.

10.1021/ma001745s CCC: $20.00
Published on Web 03/27/2001

utilizes functionalized ligands as initiators to prepare polymers with tailored binding sites. Chelation of the resulting macroligands to metal ions leads to metal-centered linear and star-shaped polymers by a convergent approach.[11−13]

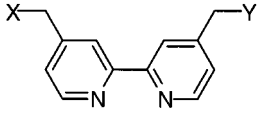

1 bpyCH$_2$Cl; X = Cl; Y = H
2 bpy(CH$_2$Cl)$_2$; X,Y= Cl
3 bpy(CH$_2$OH)$_2$; X,Y = OH
4 bpy(C$_{13}$H$_{27}$)$_2$; X,Y = -C$_{12}$H$_{25}$

Although significant advances have been made in atom transfer radical polymerization (ATRP) with organic compounds as monomers, initiators, and terminators,[14,15] far less is known about the tolerance of ATRP for metal-containing reagents. Preliminary investigations[8,11] revealed that the chloromethylbipyridine ligands **1**[16] and **2**[17] and some of their Ru(II) complexes, [Ru(bpy)$_n${bpy(CH$_2$Cl)$_2$}$_{3-n}$](PF$_6$)$_2$, **5** (n = 2), **6** (n = 1), and **7a** (n = 0),[18] are viable initiators for the polymerization of styrene using Cu bpy[19] or Cu chelating amine[20] catalyzed ATRP developed by Matyjaszewski and co-workers. Elaborating upon previously communicated results,[8] this study explores in greater detail the ATRP of styrene with both bipyridine ligand and Ru metalloinitiators. Kinetic experiments were performed and reaction parameters were varied (Figure 1) in order to determine the conditions for preparing Ru-containing polystyrenes with molecular weight control. Different counterions (**7b**), ancillary ligands (**10, 12**), and solvents (anisole, DMF) were used in order to improve solubility of metal complex reagents in ATRP reaction media. The diversity of polymer architectures anticipated with these reagents is illustrated in Figure 2.

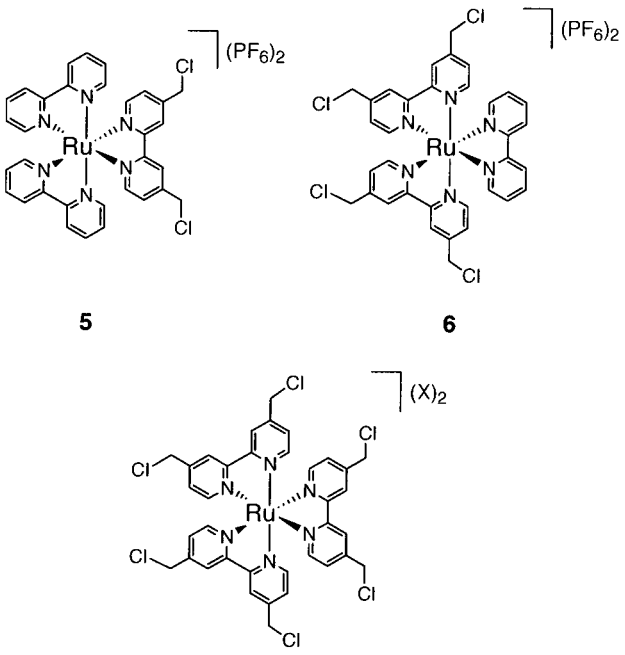

5 **6**

7a X = PF$_6^-$
7b X = BAr'$_4^-$

The fact that the metalloreagents are multifunctional presents additional challenges for attaining "well-defined" materials by ATRP. Others have noted that the incidence of termination through polymer chain coupling increases with the number of initiator sites and that this side reaction becomes more pronounced as the polymerization progresses.[21−25] In some cases, this issue was addressed with high monomer loading, by stopping polymerizations at low monomer conversion and by using less than 1 equiv of catalyst per initiator site, thus keeping the concentration of radicals low. The particular ATRP catalyst and whether reactions are run in bulk monomer or in the presence of solvent can also play a role. Hence, some of these strategies were explored for styrene polymerizations with metalloinitiators.

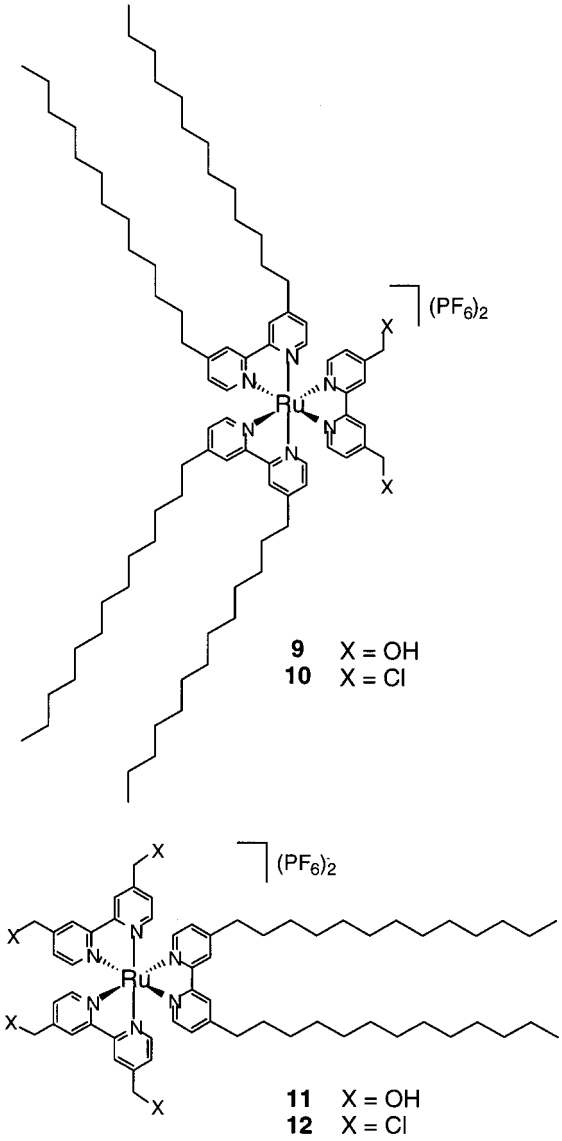

9 X = OH
10 X = Cl

11 X = OH
12 X = Cl

Experimental Section

Materials. Styrene (Acros, 99.0%) was passed through a column of neutral alumina and distilled from CaH$_2$ prior to use. RuCl$_3$·xH$_2$O (Strem, 99.9%), CuCl (Aldrich, 98+%), and 1,1,4,7,10,10-hexamethyltriethylenetetraamine (HMTETA) (Aldrich, 97.0%) were used as received. CuBr (Aldrich, 98.0%) was purified as described in the literature using acetic acid and EtOH.[26] The ruthenium complexes [Ru(bpy)$_n${bpy(CH$_2$Cl)$_2$}$_{3-n}$](PF$_6$)$_2$ (**5**, **6**, **7a**),[18] 4,4′-bis(hydroxymethyl)-2,2′-bipyridine[27] (**3**), and 4,4′-bis(tridecyl)-2,2′-bipyridine[28] (**4**) were prepared as previously described.

Instrumentation. ^{1}H NMR spectra were acquired on a GE QE 300 MHz spectrometer and were referenced vs the solvents indicated. Tentative peak assignments are provided for the respective compounds. Molecular weight of polymers were

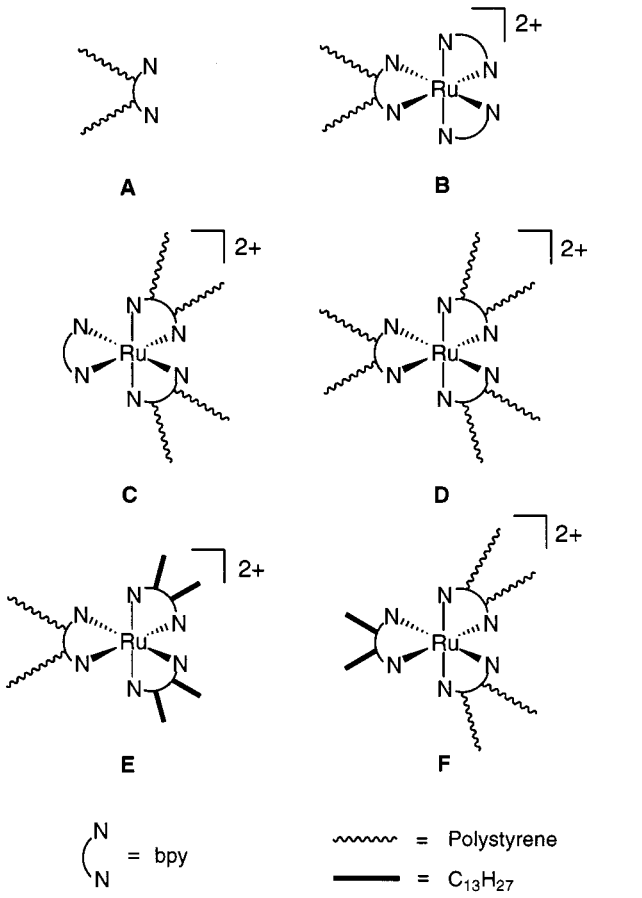

A $bpyPS_2$
B $[Ru(bpy)_2(bpyPS_2)]^{2+}$
C $[Ru(bpy)(bpyPS_2)_2]^{2+}$
D $[Ru(bpyPS_2)_3]^{2+}$
E $[Ru\{bpy(C_{13}H_{27})_2\}_2(bpyPS_2)]^{2+}$
F $[Ru\{bpy(C_{13}H_{27})_2\}(bpyPS_2)_2]^{2+}$

Figure 2. Representative polystyrene architectures obtainable with ligand and metal complex initiators.

determined by gel permeation chromatography (GPC) in $CHCl_3$ (~25 °C; flow rate 1.0 mL/min) using Hewlett-Packard series 1100 instrumentation equipped with a vacuum degasser and diode array detector with Polymer Labs 5 μ "Mixed-C" guard and GPC columns (2). Wyatt Technology Corporation DAWN multiangle laser light scattering (MALLS) (5 mW polarized He−Ne laser, $\lambda = 633$ nm) and Optilab refractive index (RI) detectors with accompanying Astra software were utilized. Refractive index increments (d*n*/d*c* values) were measured in $CHCl_3$ ($\lambda = 633$ nm, $T = 40$ °C; d*n*/d*c* = 0.145 mL/g). Differential scanning calorimetry measurements were performed using a TA Instruments DSC 2920 modulated DSC (MDSC). Analysis was performed in modulated mode (under N_2, amplitude = ±1 °C; period = 60 s; heating rate = 5 °C/min; range = 50−300 °C (cycled 3 times). Reported values of thermal events are from the second heating cycle and the reversing heat flow curve (T_g = the midpoint of the change in the heat capacity) unless otherwise indicated. UV/vis spectra were recorded using a Hewlett-Packard 8453 UV/vis spectrophotometer with UV/vis Chemstation Rev.A.02.05 software.

$[Ru\{bpy(CH_2Cl)_2\}_3](BAr'_4)_2$ (7b). $[Ru\{bpy(CH_2Cl)_2\}_3](PF_6)_2$ (0.500 g, 0.435 mmol) and sodium tetraarylborate ($NaB\{3,5\text{-}(CF_3)_2C_6H_3\}_4$) (0.770 g, 0.869 mmol) were dissolved in THF (10 mL) and stirred for 16 h, before removing the solvent in vacuo. The orange residue was dissolved in CH_2Cl_2, filtered through Celite, and concentrated in vacuo. The resulting solid was triturated with H_2O (50 mL), collected by filtration, and dried in vacuo: 1.02 g, 89%. ^1H NMR (CD_3CN): δ 8.67 (s, 6 H, H-3, H-3′), 7.84 (m, 30 H, H-6, H-6′ and $B\{3,5\text{-}(CF_3)C_6H_3\}_4$), 7.56 (m, 6 H, H-5, H-5′), 4.84 (s, 12 H, CH_2Cl). UV/vis (CH_3CN): λ_{max} (ϵ) = 460 nm (14 860 M^{-1} cm^{-1}). Anal. Calcd for $C_{100}H_{54}N_6Cl_6B_2F_{48}Ru$: C, 46.43; H, 2.10; N, 3.25. Found: C, 46.05; H, 2.12; N, 2.88.

$[Ru\{bpy(C_{13}H_{27})_2\}_3](PF_6)_2$ (8). $RuCl_3 \cdot xH_2O$ (0.200 g, 0.794 mmol), $bpy(C_{13}H_{27})_2$ (1.43 g, 2.75 mmol), hydroquinone (0.244 g, 2.22 mmol), and EtOH (30 mL) were combined and heated at reflux for 16 h. The red maroon solution was cooled to room temperature and filtered, and then solid $NaPF_6$ (0.745 g, 4.44 mmol) was added to precipitate a red solid. After stirring for 16 h, the solid was collected by filtration, purified by precipitation from CH_2Cl_2/hexanes, and dried under vacuum: 0.920 g, 53%. ^1H NMR ($CDCl_3$): δ 8.07 (s, 6 H, H-3, H-3′), 7.56 (d, J = 6 Hz, 6 H, H-6, H-6′), 7.29 (d, J = 6 Hz, 6 H, H-5, H-5′), 2.79 (t, J = 8 Hz, 12 H, $CH_2(CH_2)_{11}CH_3$), 1.78−1.61 (m, 12 H, $CH_2CH_2(CH_2)_{10}CH_3$), 1.43−1.11 (m, 120 H, $CH_2CH_2(CH_2)_{10}CH_3$), 0.86 (t, J = 7 Hz, 18 H, $CH_2CH_2(CH_2)_{10}CH_3$). UV/vis (CH_3CN): λ_{max} (ϵ) = 462 nm (15 980 M^{-1} cm^{-1}). UV/vis ($CHCl_3$): λ_{max} (ϵ) = 462 nm (18 320 M^{-1} cm^{-1}). Anal. Calcd for $C_{108}H_{180}N_6P_2F_{12}Ru$: C, 66.40; H, 9.29; N, 4.30. Found: C, 66.74; H, 9.20; N, 4.09.

$[Ru\{bpy(C_{13}H_{27})_2\}_2\{bpy(CH_2OH)_2\}](PF_6)_2$ (9). $RuCl_3 \cdot xH_2O$ (0.250 g, 0.993 mmol), $bpy(C_{13}H_{27})_2$, **4** (1.06 g, 2.04 mmol), hydroquinone (0.286 g, 2.60 mmol), and LiCl (1.30 g, 30.7 mmol) were combined with MeOH (30 mL) and DME (15 mL). The purple mixture was refluxed for 5 h and concentrated in vacuo. The resulting maroon solid was dissolved in CH_2Cl_2 (75 mL), washed with H_2O (3 × 100 mL), and the organic layer was concentrated in vacuo. $Bpy(CH_2OH)_2$ (0.334 g, 1.74 mmol) and an EtOH (100 mL)/butanol (25 mL) mixture were added to the residue, and the resulting deep maroon solution was heated at reflux for 16 h. After cooling to room temperature, the red-orange solution was concentrated in vacuo to a red oil (~2 mL), and CH_2Cl_2 (50 mL) was added. The organic layer was washed with H_2O (3 × 50 mL) and concentrated in vacuo. The resulting red solid was dissolved in a minimal amount of EtOH (~12 mL) and filtered through Celite before addition of $NaPF_6$(s) (0.381 g, 2.27 mmol). After stirring for ~15 h, the red solid thus produced was collected by filtration, washed with H_2O, and dried in vacuo: 1.43 g, 84%. ^1H NMR (CD_3CN): δ 8.46 (s, 2 H, $bpy(CH_2OH)_2$ H-3, H-3′), 8.32 (s, 4 H, $bpy(C_{13}H_{27})_2$ H-3, H-3′), 7.59 (d, J = 6 Hz, 2 H, $bpy(CH_2OH)_2$ H-6, H-6′), 7.51 (m, 4 H, $bpy(C_{13}H_{27})_2$ H-6, H-6′), 7.31 (d, J = 6 Hz, 2 H, $bpy(CH_2OH)_2$ H-5, H-5′), 7.19 (d, J = 6 Hz, 4 H, $bpy(C_{13}H_{27})_2$ H-5, H-5′), 4.76 (s, 4 H, CH_2OH), 2.77 (t, J = 7.2 Hz, 8 H, $CH_2(CH_2)_{11}CH_3$), 1.68 (m, 8 H, $CH_2CH_2(CH_2)_{10}CH_3$), 1.24 (m, 82 H, $CH_2CH_2(CH_2)_{10}CH_3$, OH), 0.86 (t, J = 6.6 Hz, 12 H, $CH_2(CH_2)_{11}CH_3$). UV/vis ($CHCl_3$): λ_{max} (ϵ) = 463 nm (17 744 M^{-1} cm^{-1}). Anal. Calcd for $C_{84}H_{132}N_6O_2P_2F_{12}Ru$: C, 61.17; H, 8.08; N, 5.09. Found: C, 61.15; H, 8.34; N, 4.61.

$[Ru\{bpy(C_{13}H_{27})_2\}_2\{bpy(CH_2Cl)_2\}](PF_6)_2$ (10). Chlorination of the alcohol complex **9** was effected as previously described:[18] 0.160 g, 78%. ^1H NMR (CD_3CN): δ 8.62 (s, 2 H, $bpy(CH_2Cl)_2$ H-3, H-3′), 8.36 (s, 4 H, $bpy(C_{13}H_{27})_2$ H-3, H-3′), 7.69 (d, J = 5 Hz, 2 H, $bpy(CH_2Cl)_2$ H-6, H-6′), 7.49 (m, 4 H, $bpy(C_{13}H_{27})_2$ H-6, H-6′), 7.41 (d, J = 6 Hz, 2 H, $bpy(CH_2Cl)_2$ H-5, H-5′), 7.20 (d, J = 6 Hz, 4 H, $bpy(C_{13}H_{27})_2$ H-5, H-5′), 4.80 (s, 4 H, CH_2Cl), 2.78 (t, J = 7 Hz, 8 H, $CH_2(CH_2)_{11}CH_3$), 1.65 (m, 8 H, $CH_2CH_2(CH_2)_{10}CH_3$), 1.24 (br m, 80 H, $CH_2CH_2(CH_2)_{10}CH_3$), 0.86 (t, J = 7 Hz, 12 H, $CH_2(CH_2)_{11}CH_3$). UV/vis ($CHCl_3$): λ_{max} (ϵ) = 462 nm (13 140 M^{-1} cm^{-1}). Accurate FAB high-resolution mass spectrum for $[Ru\{bpy(C_{13}H_{27})_2\}_2\{bpy(CH_2Cl)_2\}](PF_6)^+$ (*m*/*z*): calcd for $C_{84}H_{130}N^{35}Cl^{37}ClPF_6{}^{100}Ru$, 1539.8320; found, 1539.8366.

$[Ru\{bpy(C_{13}H_{27})_2\}\{bpy(CH_2OH)_2\}_2](PF_6)_2$ (11). $RuCl_3 \cdot xH_2O$ (0.200 g, 0.794 mmol), $bpy(CH_2OH)_2$, **3**, (0.340 g, 1.57 mmol), hydroquinone (0.22 g, 2.00 mmol), and LiCl (1.01 g, 23.8 mmol) were combined with MeOH (30 mL) and DME (15 mL). After heating at reflux for 5 h, the resulting purple mixture was cooled to room temperature, concentrated to ~3 mL, and poured into H_2O (50 mL). The aqueous solution was washed with CH_2Cl_2 (5 × 50 mL), filtered through Celite, and concentrated to a maroon oil (~3 mL). The ligand, $bpy(C_{13}H_{27})_2$, **4**, (0.830 g, 1.59 mmol), and EtOH (50 mL) were added to the aqueous mixture which was heated at reflux for 16 h. After

cooling to room temperature, the cloudy red-orange reaction mixture was filtered through a glass frit and concentrated in vacuo. The resulting residue was dissolved in a 1:1 CH_3CN:MeOH solvent mixture (25 mL each) which was washed with pentane to remove excess bpy($C_{13}H_{27}$)$_2$. The CH_3CN/MeOH layer was concentrated in vacuo. The resulting residue was redissolved in EtOH (10 mL) for the addition of solid $NaPF_6$ (0.270 g, 1.6 mmol). After stirring for 15 h, the red solid was collected by filtration and washed with H_2O. The crude solid was purified by precipitation from CH_2Cl_2/hexanes: 0.460 g, 42%. ^{1}H NMR (CD_3CN): δ 8.48 (s, 4 H, bpy(CH_2OH)$_2$ H-3, H-3′), 8.33 (s, 2 H, bpy($C_{13}H_{27}$)$_2$ H-3, H-3′), 7.61 (t, J = 6 Hz, 4 H, bpy(CH_2OH)$_2$ H-6, H-6′), 7.54 (d, J = 5.4 Hz, 2 H, bpy($C_{13}H_{27}$)$_2$ H-6, H-6′), 7.30 (m, 4 H, bpy(CH_2OH)$_2$ H-5, H-5′), 7.19 (d, J = 5.4 Hz, 2 H, bpy($C_{13}H_{27}$)$_2$ H-5, H-5′), 4.76 (s, 8 H, CH_2OH, 2.78 (t, J = 6.5 Hz, 4 H, $CH_2(CH_2)_{11}CH_3$), 1.68 (m, 4 H, $CH_2CH_2(CH_2)_{10}CH_3$), 1.24 (br m, 42 H, $CH_2CH_2(CH_2)_{10}CH_3$ and OH), 0.86 (t, J = 7 Hz, 6 H, $CH_2(CH_2)_{11}CH_3$). UV/vis ($CHCl_3$): λ_{max} (ϵ) = 460 nm (13 010 M^{-1} cm^{-1}). Accurate FAB high-resolution mass spectrum for [Ru{bpy($C_{13}H_{27}$)$_2$}{bpy(CH_2OH)$_2$}$_2$](PF_6)$^+$ (m/z): calcd for $C_{60}H_{84}N_6O_4PF_6{}^{102}$Ru, 1199.5344; found, 1199.5294.

[Ru{bpy($C_{13}H_{27}$)$_2$}{bpy(CH_2Cl)$_2$}$_2$](PF_6)$_2$ (12). The tetraol **11** was converted to the chloride **12** as previously described[18] with the following exceptions. The compound was purified by dissolving in CH_2Cl_2 and washing with H_2O (3 times) followed by precipitation from CH_2Cl_2/hexanes: 0.393 g, 75%. ^{1}H NMR (CD_3CN): δ 8.72 (s, 4 H, bpy(CH_2Cl)$_2$ 3, 3′ H), 8.41 (s, 2 H, bpy($C_{13}H_{27}$)$_2$ H-3, H-3′), 7.69 (m, 4 H, bpy(CH_2Cl)$_2$ H-6, H-6′), 7.48 (m, 6 H, bpy($C_{13}H_{27}$)$_2$ H-6, H-6′ and bpy(CH_2Cl)$_2$ H-5, H-5′), 7.23 (m, 2 H, bpy($C_{13}H_{27}$)$_2$ H-5, H-5′), 4.82 (s, 8 H, CH_2Cl), 2.78 (t, J = 6.6 Hz, 4 H, $CH_2(CH_2)_{11}CH_3$), 1.68 (m, 4 H, $CH_2CH_2(CH_2)_{10}CH_3$), 1.24 (br m, 40 H, $CH_2CH_2(CH_2)_{10}CH_3$), 0.86 (t, J = 7 Hz, 6 H, $CH_2(CH_2)_{11}CH_3$). UV/vis ($CHCl_3$): λ_{max} (ϵ) = 459 nm (15 480 M^{-1} cm^{-1}). (See Supporting Information for ^{1}H and ^{13}C NMR spectral data.)

Representative Procedure for Kinetics Studies. *Method A.* In a glovebox, a stock solution of CuCl (0.0348 g, 0.352 mmol), bpy($C_{13}H_{27}$)$_2$ (0.367 g, 0.704 mmol), and styrene (8.10 mL) was prepared, and then anisole (14% v/v vs styrene) (or DMF; 10% v/v vs styrene) was added. The dark-brown mixture was stirred until a homogeneous solution was achieved (∼20 min), and then a portion of it (5.45 g) was delivered to a 25 mL Kontes tube containing **7a** (0.048 g, 0.041 mmol) such that styrene:initiator Cl = 200:1. The mixture was sealed under N_2 and removed from the box. The tube was immersed in an oil bath maintained at 110 °C, and the initial time was recorded. Aliquots (∼0.5−0.1 mL) were removed at the designated times for distribution to two separate vials. One fraction was placed under high vacuum (∼0.1 Torr) until constant mass was achieved (≥2 days) for determination of monomer conversion by gravimetric analysis. The other portion was quenched with THF immediately. The mixture was passed through a plug of neutral alumina, concentrated to a solid in vacuo, and purified by precipitation from CH_2Cl_2/hexanes to yield orange solids that were characterized by GPC. *Method B.* Kinetics reactions with the CuBr/HMTETA catalyst were run with similar reagent loadings, with the following changes to molecular weight and percent monomer conversion determination. At the designated time, aliquots were removed and diluted in THF. Percent monomer conversion was determined by GC/MS by comparison of the areas corresponding to the styrene and anisole peaks. Crude polymers were purified by passage of the THF solutions through alumina before GPC molecular weight analysis.

Preparative Scale Polymerizations. Polymerizations with CuBr/HMTETA were run for 2 h, such that ∼2 g of polymer could be obtained at ∼30% conversion, as estimated from M_n vs percent monomer conversion studies. A representative preparative scale reaction is provided for Ru{bpy($C_{13}H_{27}$)$_2$}$_2${bpy(CH_2Cl)$_2$}](PF_6)$_2$ (**10**). In a glovebox, styrene (14.35 g, 0.137 mol), CuBr (0.098 g, 0.683 mmol), HMTETA (0.158 g, 0.686 mmol), and anisole (2.30 g; 14% v/v vs styrene) were combined and stirred until a homogeneous solution was attained (∼30−45 min). A portion of the resulting dark brown solution (8.33 g) was transferred to a Kontes tube containing the appropriate preweighed difunctional initiator **10** (0.284 g, 0.168 mmol) to achieve the following molar ratio: [styrene]/[initiator Cl]$_0$/[CuBr]/[HMTETA] = 200/1/1/1. The tube was sealed, removed from the glovebox, and immersed in an oil bath maintained at 110 °C. After 2 h, the polymerization was removed from the oil bath and quenched with THF. The orange solution was passed through a neutral alumina plug to remove the copper catalyst. Precipitation from THF/MeOH followed by CH_2Cl_2/hexanes further purified the polymer. The resulting orange powder was collected and dried in vacuo: 1.84 g, 68% (corrected for unreacted styrene). GPC: M_n = 22 000, M_w = 26 400, PDI = 1.20. UV/vis ($CHCl_3$): λ_{max} (ϵ) = 464 nm (20 120 M^{-1} cm^{-1}). ^{1}H NMR ($CDCl_3$): δ 7.2−6.9 (br m, −C_6H_5). 6.7−6.3 (br m, −C_6H_5), 2.1−1.2 (br m, −CHPhCH_2−). (A peak corresponding to the −CH_2− groups on the $C_{13}H_{27}$ side chains is evident at 1.25 ppm.)

Determination of Ru Content by UV/vis Spectroscopy. Polymers were prepared as described above for M_n vs conversion studies using the CuCl/2bpy($C_{13}H_{27}$)$_2$ catalyst system. Samples were purified by passage through neutral alumina and precipitation from THF/MeOH and CH_2Cl_2/hexanes. A portion of the orange solid was dissolved in $CHCl_3$, the resulting orange-red solution was filtered through paper, and an aliquot of the filtrate fraction was used for molecular weight determination by GPC. The remainder of the solution was transferred to a tared vial, and the solvent was removed and samples were dried in vacuo for at least 2 days. Using the dry sample and the M_n for it as determined by GPC, 10−25 μM $CHCl_3$ solutions were prepared, and UV/vis spectra were recorded.

Polymerizations in Bulk Styrene and Corresponding Control Reactions. Reactions were performed as described above for M_n vs conversion studies but without addition of solvent. Instead of aliquot removal from a single tube, independent reactions were quenched at different times and polymer products were analyzed by GPC. Typical loadings were as previously described[8] (initiator Cl/CuCl/bpy($C_{13}H_{27}$)$_2$/styrene = 1/1/2/174). Reagent loadings for various control reactions are indicated below: (a) Autopolymerization of styrene. (b) Polymerization of styrene in the presence of [Ru(bpy)$_3$](PF_6)$_2$. Eight Kontes tubes each containing [Ru(bpy)$_3$](PF_6)$_2$ (0.022 g, 0.025 mmol) were charged with styrene (0.50 mL, 4.36 mmol). This experiment was also conducted at higher loadings of Ru reagent. (c) Polymerization of styrene in the presence of [Ru(bpy)$_3$](PF_6)$_2$, CuCl, and bpy($C_{13}H_{27}$)$_2$. A stock solution of styrene (5.00 mL, 43.6 mmol) containing CuCl (0.050 g, 0.050 mmol) and bpy($C_{13}H_{27}$)$_2$ (0.522 g, 0.100 mmol) was prepared for distribution to 10 Kontes tubes, each containing [Ru(bpy)$_3$](PF_6)$_2$ (0.022 g, 0.025 mmol). This experiment was also conducted at higher loadings of Ru reagent. (d) Polymerization of styrene in the presence of [Ru{bpy($C_{13}H_{27}$)$_2$}$_3$](PF_6)$_2$, **8**. [Ru{bpy($C_{13}H_{27}$)$_2$}$_3$](PF_6)$_2$ (0.494 g, 0.253 mmol) was dissolved in styrene (5.0 mL, 43.6 mmol) and distributed equally to 10 Kontes tubes. This experiment was also conducted at higher loadings of Ru reagent. (e) Polymerization of styrene in the presence of [Ru{bpy($C_{13}H_{27}$)$_2$}$_3$](PF_6)$_2$, CuCl, and bpy($C_{13}H_{27}$)$_2$. A stock solution of styrene (5.00 mL, 43.6 mmol) containing CuCl (0.050 g, 0.050 mmol), bpy($C_{13}H_{27}$)$_2$ (0.522 g, 0.100 mmol), and [Ru{bpy($C_{13}H_{27}$)$_2$}$_3$](PF_6)$_2$ (0.494 g, 0.253 mmol) was distributed equally to 10 Kontes tubes. (f) Polymerization of styrene in the presence of CuCl and bpy($C_{13}H_{27}$)$_2$. A stock solution of styrene (4.50 mL, 39.3 mmol) containing CuCl (0.045 g, 0.045 mmol) and bpy($C_{13}H_{27}$)$_2$ (0.471 g, 0.090 mmol) was distributed equally to nine Kontes tubes. (g) Polymerization of styrene with bpy(CH_2Cl)$_2$ in the presence of CuCl but without bpy($C_{13}H_{27}$)$_2$. Styrene (0.50 mL, 4.36 mmol) was added to five tubes each containing bpy(CH_2Cl)$_2$ (25.0 mg, 0.100 mmol) and CuCl (5.00 mg, 0.050 mmol). (h) Polymerization of styrene with [Ru{bpy(CH_2Cl)$_2$}$_3$](PF_6)$_2$, **7a**, and no copper catalyst. Styrene (2.00 mL, 17.5 mmol) was added to five tubes each containing [Ru{bpy(CH_2Cl)$_2$}$_3$](PF_6)$_2$ (5.00 g, 0.042 mmol) under nitrogen.

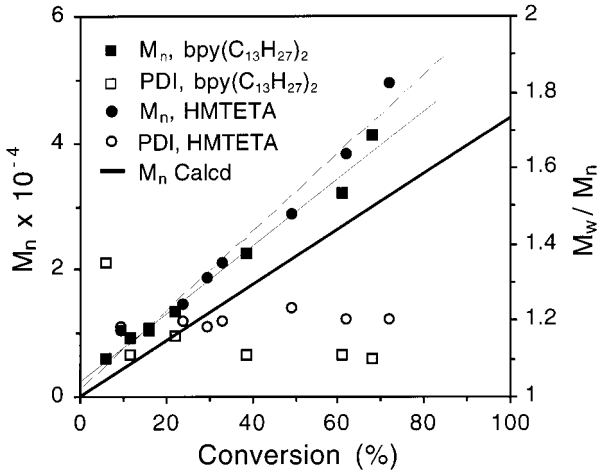

Figure 3. Comparison of M_n vs % monomer conversion plots and polydispersities for the atom transfer radical polymerization of styrene using the difunctional initiator, bpy(CH_2Cl)$_2$, **2**, and the CuCl/2bpy($C_{13}H_{27}$)$_2$ and CuBr/HMTETA catalyst systems (bpy(CH_2Cl)$_2$/Cu/L/styrene: L = bpy($C_{13}H_{27}$)$_2$: 1/2/4/400, L = HMTETA: 1/2/2/400; 14% anisole (v/v with styrene); 110 °C).

Results and Discussion

For preparative scale reactions (~0.5−2 mL of styrene), polymers with narrow molecular weight distributions are obtained when styrene is polymerized with the ligand initiators,[8,11−13] bpy(CH_2Cl)$_n$ **1** and **2**, or their Ru metal complexes, **5**, **6**, and **7a** using CuCl and a solubilizing bipyridine ligand, 4,4′-bis(tridecyl)-2,2′-bipyridine, bpy($C_{13}H_{27}$)$_2$, **4**, as the ATRP catalyst system in bulk monomer.[8] In this study, detailed kinetics experiments were performed using comparable reaction conditions. A variety of different methods were screened in order to determine the extent to which these polymerizations are controlled. Polymerizations were run in bulk styrene in multiple reaction tubes such that the entire mixture per tube might be quenched at a given time. They were also performed in a single tube with aliquot removal at designated times. Monomer conversion was measured by GC with anisole added as an internal standard, or it was determined by gravimetric analysis. Results were most consistent and reproducible when reactions were performed with aliquot removal from a single tube, monomer conversion was determined by the gravimetric methods, and a small amount of anisole (14% v/v vs styrene) was added to the polymerizations. Addition of solvent lowered the viscosity slightly as compared with those run in bulk styrene, thus facilitating aliquot removal at high monomer conversion. The solubility of the initiators may also be enhanced to a small extent. Hence, these optimal conditions were employed for all kinetics experiments reported in this study unless otherwise indicated.

Reactions with the soluble ligand initiator, bpy(CH_2Cl)$_2$, **2**, to form bpyPS$_2$ (Figure 2A) were reasonably controlled. For the CuCl/2bpy($C_{13}H_{27}$)$_2$ catalyst system, M_n vs percent conversion plots are linear up to ~60% conversion, and polydispersity indices (PDIs) are typically low (<1.2) (Figure 3). Above this point, molecular weights deviate more dramatically from targeted values, suggesting that polymer coupling by radical recombination may be occurring. Experimental M_n values are generally slightly higher than calculated ones, which suggests either poor initiator efficiency or, more likely for this soluble initiator, the destruction of some initiator sites during the establishment of equilibrium in the early stages of these reactions.[29] Representative molecular weight data and initiator efficiencies for **2** and other polymers are provided in Table 1. First-order kinetics plots are also linear at low monomer conversion, as is expected for a controlled polymerization (Figure 4).

In general, reactions of bpy(CH_2Cl)$_2$ with the Cu/HMTETA catalyst were slightly less controlled than those with the CuCl/2bpy($C_{13}H_{27}$)$_2$ system. Again, reasonable molecular weight control is observed up to ~60% conversion; however, radical coupling at higher conversion is more significant in this case (Figure 3). The higher PDIs observed could be indicative of increased radical coupling and possibly to faster propagation relative to initiation for the Cu/HMTETA reaction, which also exhibits a longer induction period. Interestingly, the reaction rates were slower for the quadridentate amine catalyst than with bpy($C_{13}H_{27}$)$_2$, which is contrary to what is normally observed; typically, halide abstraction and formation of the Cu(II) state are favored for the former stronger donor ligand.[20] (See Table 2, entries 13 and 14, for comparison of apparent rate constants for these reactions along with data for other initiators.) This could be due, in part, to the fact that bpy(CH_2Cl)$_2$ may function both as an initiator and as a ligand for copper. It seems quite plausible that the initiator, bpy(CH_2Cl)$_2$, competes more effectively with the bidentate α-diimine bpy donor for coordination to copper, bpy($C_{13}H_{27}$)$_2$, than it does with HMTETA, a quadridentate ligand with a stronger amine ligand field. If coordination of bpy(CH_2Cl)$_2$ to Cu serves to activate the initiator for polymerization, this could account for the unusual trend in reaction rates. Attempts to take advantage of this dual role for bpy(CH_2Cl)$_2$, by polymerizing styrene in the presence of bpy(CH_2Cl)$_2$ using CuCl but no bpy($C_{13}H_{27}$)$_2$ or HMTETA, also yielded polymers with narrow molecular weight distributions. However, the reactions were heterogeneous and not entirely controlled. A red solid, presumably the Cu(I) complex of bpy(CH_2Cl)$_2$, precipitated from the reaction mixture upon combination of bpy initiator **2** with CuCl.

Polymers produced from metalloinitiators **5**−**7a** also have low polydispersities (~1.2) for both CuCl/2bpy($C_{13}H_{27}$)$_2$ and CuBr/HMTETA catalyst systems when anisole is added to the reaction mixtures. However, molecular weights are typically higher than the targeted values, often by as much as a factor of 2 for the Cu/HMTETA catalyzed reactions. Comparison of initiator efficiencies for these two different reagent sets (Table 1, entries 1 and 2; 3 and 4; 5 and 7) along with other data indicated that reactions with CuCl/2bpy($C_{13}H_{27}$)$_2$ were slightly better controlled. For CuCl/2bpy($C_{13}H_{27}$)$_2$ catalyzed reactions, molecular weights increase in an approximately linear fashion with percent monomer conversion, although M_n vs percent monomer conversion plots intercept the *y*-axis at molecular weights considerably higher than anticipated on the basis of initiator molar masses, indicative of poor initiation. Inspection of the first-order kinetics plots revealed induction periods for many of these reactions, regardless of the catalyst (e.g., for **5**: CuCl/2bpy($C_{13}H_{27}$)$_2$: ~50 min (Figure 5); CuBr/HMTETA: ~30 min). The dicationic metalloinitiators (**5**, **6**, **7a**) are not entirely soluble in bulk styrene.[8] Under these conditions, red-orange oils presumed to be insoluble Ru complex were sometimes evident at the bottom of the reaction vessels after polymerization and are collected at the top of alumina

Table 1. Comparison of Initiator Efficiencies for Selected Polymers Prepared from bpy(CH_2Cl)$_2$, 2, and Metalloinitiators [Ru(bpy)$_n$(bpy(CH_2Cl)$_2$}$_m$](PF_6)$_2$ (5−7a) and [Ru{bpy($C_{13}H_{27}$)$_2$}$_n$(bpy(CH_2Cl)$_2$}$_m$](PF_6)$_2$ (10 and 12) Using CuCl/2bpy($C_{13}H_{27}$)$_2$ or CuBr/HMTETA Catalyst Systems

entry	initiator	[styrene]$_0$/[initiator]$_0$	catalyst[a]	monomer conversion[b] (%)	calcd $M_n \times 10^{-3}$	M_n[c] $\times 10^{-3}$	M_w/M_n	I_{eff}[d]
1	**5**	400	C13bpy	41.5	18.5	27.8	1.21	0.67
2	**5**	400	HMTETA	40.2	17.7	37.0	1.19	0.48
3	**6**	800	C13bpy	31.6	27.4	49.0	1.20	0.56
4	**6**	800	HMTETA	28.1	24.5	41.6	1.17	0.59
5	**7a**	1200	C13bpy	21.8	28.4	55.9	1.19	0.51
6	**7a**	1200	C13bpy[e]	22.5	29.3	41.3	1.09	0.71
7	**7a**	1200	HMTETA	24.4	31.6	72.1	1.24	0.44
8	**10**	400	C13bpy	24.9	12.1	14.9	1.08	0.81
9	**10**	400	HMTETA	26.5	12.7	16.1	1.16	0.79
10	**12**	800	C13bpy	33.2	29.2	45.9	1.20	0.64
11	**12**	800	HMTETA	33.7	29.5	39.9	1.20	0.74
12	**2**	400	C13bpy	61.2	27.0	31.8	1.11	0.85
13	**2**	400	HMTETA	61.8	27.3	38.3	1.20	0.71

[a] C13bpy = CuCl/2bpy($C_{13}H_{27}$)$_2$; HMTETA = CuBr/HMTETA in 14% anisole (v/v vs styrene). [b] Determined by GC/MS for HMTETA and gravimetric analysis for C13bpy. [c] Determined by GPC with RI and MALLS detection. [d] I_{eff} = initiator efficiency = calcd M_n/M_n. [e] In 10% DMF (v/v vs styrene).

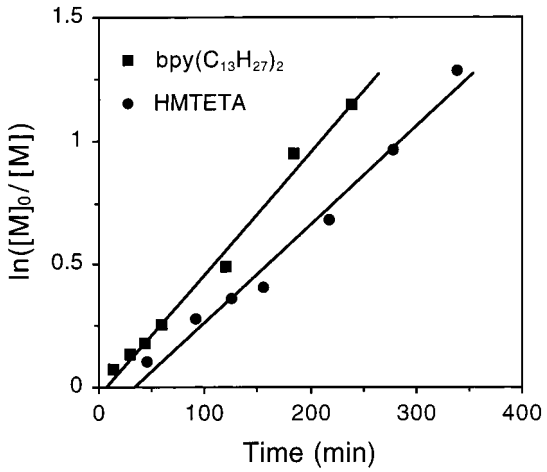

Figure 4. Comparison of first-order kinetics plots for the ATRP of styrene with the difunctional ligand initiator bpy(CH_2Cl)$_2$, **2**, using the CuCl/2bpy($C_{13}H_{27}$)$_2$ and CuBr/HMTETA catalyst systems. (For reagent loadings, see Figure 3.)

columns during product purification. The fact that polydispersities were typically very low and remained roughly constant for CuCl/2bpy($C_{13}H_{27}$)$_2$ catalyzed reactions initiated with **5**−**7a**, suggested that the initiators do not gradually dissolve throughout the course of the polymerization. Rather, they must become even less soluble as polymerization commences and polystyrene is produced.

For CuBr/HMTETA reactions, in contrast, molecular weight distributions are not constant but instead increase markedly as the reaction progresses. This could signal slow and gradual initiation throughout the course of the reaction, a greater incidence of radical coupling, or possibly competing thermal autopolymerization of styrene. At high monomer conversions, GPC chromatograms revealed high molecular weight shoulders on the major polymer fraction for all metalloinitiators. This feature was particularly prominent as the number of initiator sites increased, and it was more pronounced for reactions with CuBr/HMTETA than for those with the CuCl/2bpy($C_{13}H_{27}$)$_2$ catalyst system. Moreover, in-line UV/vis analysis indicated the presence of Ru chromophores in these higher molecular weight fractions, which is not anticipated for polystyrene initiated thermally. Although slow initiation is very likely responsible for some broadening of the PDIs, the appearance of discrete shoulders on the high, not low, molecular weight side of GPC peaks as the reaction progresses seems more most consistent with increased radical coupling at high conversion.

Table 2. Rate Constants for the Atom Transfer Radical Polymerization of Styrene with bpy(CH_2Cl)$_2$ and Various Metalloinitiators[a]

entry	initiator	catalyst[b]	[initiator]$_0$ (mM)	k_{app}[c] ($s^{-1} \times 10^{-5}$)
1	**5**	C13bpy	18.7	8.3
2	**5**	HMTETA	18.7	20.0
3	**6**	C13bpy	9.3	6.2
4	**6**	HMTETA	9.3	6.6
5	**7a**	C13bpy	6.2	2.5
6	**7a**	C13bpy[d]	6.5	4.5
7	**7a**	HMTETA[e]	6.2	5.2
8	**10**	C13bpy	18.7	4.2
9	**10**	HMTETA	18.7	6.3
10	**12**	C13bpy	9.3	5.7
11	**12**	C13bpy[f]	50.0	2.7
12	**12**	HMTETA	9.3	18.0
13	**2**	C13bpy	18.7	8.3
14	**2**	HMTETA	18.7	6.0

[a] [CuX]$_0$ = 37.4 mM; [styrene]$_0$ = 7.46 M; [anisole]$_0$ = 1.30 M; [styrene]$_0$/[initiator Cl]$_0$ = 200/1 unless otherwise indicated. [b] C13bpy = CuCl/2bpy($C_{13}H_{27}$)$_2$; HMTETA = CuBr/HMTETA. [c] Calculated from the slope of ln([M]$_0$/[M]) vs time plots prior to the onset of pronounced termination by radical recombination. [d] [CuX]$_0$ = 39.0 mM; [styrene]$_0$ = 7.82 M; [DMF]$_0$ = 1.29 M; [styrene]$_0$/[initiator Cl]$_0$ = 200/1. [e] [CuX]$_0$ = 18.7 mM; [styrene]$_0$ = 7.46 M; [anisole]$_0$ = 1.30 M; [styrene]$_0$/[initiator Cl]$_0$ = 200/1. [f] [CuX]$_0$ = 100.0 mM; [styrene]$_0$ = 8.72 M; [anisole]$_0$ = 0 M; [styrene]$_0$/[initiator Cl]$_0$ = 174/1.

Similar observations have been made by others with multifunctional initiators and have been ascribed to radical coupling of growing chains.[21−25] Matyjaszewski has noted that when radical concentrations are decreased by using lower catalyst loadings, termination by star−star coupling is minimized.[21] Similarly, high molecular weight shoulders were diminished when reactions with **6** and **7a** were run at half catalyst loading for CuCl/2bpy($C_{13}H_{27}$)$_2$ in bulk styrene or for CuBr/HMTETA in anisole (14% v/v vs styrene). This was not the case for reactions with CuCl/2bpy($C_{13}H_{27}$)$_2$ in styrene containing 14% anisole (v/v) (or 10% DMF); reactions run with initiator Cl/Cu loadings of 1/0.5 were less controlled than were those performed at 1:1 loadings for **6** and **7a**. As noted by others,[22] regardless of catalyst, molecular weight control is better if monomer loadings

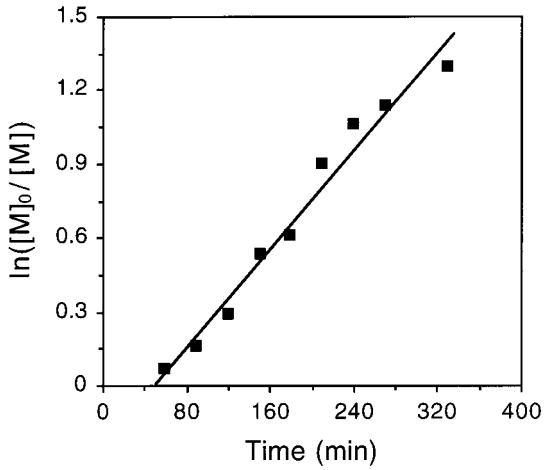

Figure 5. First-order kinetics plot for the polymerization of styrene with the difunctional metalloinitiator $[Ru(bpy)_2\{bpy(CH_2Cl)_2\}](PF_6)_2$, **5**, using the $CuCl/2bpy(C_{13}H_{27})_2$ catalyst system ($Ru/CuCl/2bpy(C_{13}H_{27})_2$/styrene: 1/2/4/400; 14% anisole (v/v with styrene); 110 °C).

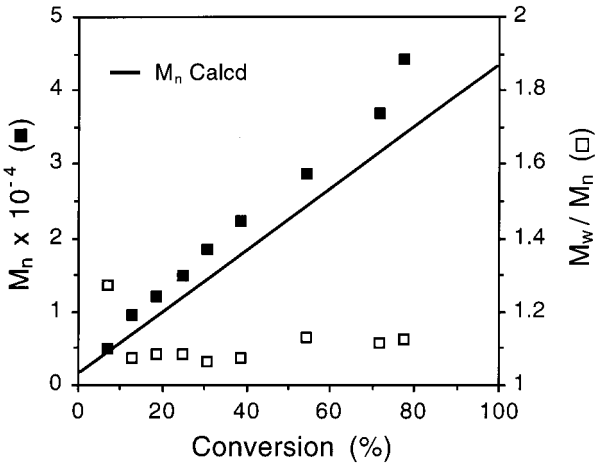

Figure 6. Number-average molecular weight vs percent monomer conversion plot and polydispersities for the polymerization of styrene in anisole using the difunctional metalloinitiator, $[Ru\{bpy(C_{13}H_{27})_2\}_2\{bpy(CH_2Cl)_2\}](PF_6)_2$ **12**, and the $CuCl/2bpy(C_{13}H_{27})_2$ catalyst system ($Ru/Cu/bpy(C_{13}H_{27})_2$/styrene = 1/2/4/400; 14% anisole (v/v with styrene); 110 °C).

are kept high and reactions are not run to high monomer conversion.

Control reactions run with styrene in the absence of initiator gave rise to rapid, uncontrolled chain growth polymerization that is characteristic of styrene autopolymerization; molecular weights of the resulting polymers were typically in the range of 400 000−600 000. Were autopolymerization a significant side reaction in ATRP with metalloinitiators, for samples collected early in the polymerization, multimodal GPC traces with well-separated peaks arising from controlled and uncontrolled reactions would be anticipated. Although in some cases small, high molecular weight Ru-free peaks were observed in GPC traces of samples which may be attributable to autopolymerization, generally this feature is distinct from the shoulders that grow as the reactions progress. Even for thermal polymerizations run in bulk styrene in the presence of Ru reagents with no initiator groups, no Ru remained associated with the polystyrene after purification. Neither $[Ru(bpy)_3](PF_6)_2$ nor the more soluble $[Ru\{bpy(C_{13}H_{27})_2\}_3](PF_6)_2$ appeared to exert any special influence upon the autopolymerization of styrene when loaded at concentrations comparable to those employed in this study for kinetics and preparative reactions. When thermal polymerizations were performed in the presence of higher loadings of **8** or Ru(II) tris(bpy) (i.e., $Ru/CuX/bpy(C_{13}H_{27})_2$/styrene = ≥2/1/2/174 or Ru/styrene = ≥2/174), certain (but not all) runs exhibited improved molecular weight control compared to reactions performed in the absence of Ru or the copper ATRP catalyst $CuCl/2bpy(C_{13}H_{27})_2$. In certain cases, the Ru reagents appeared to inhibit autopolymerization to varying extents. These observations merit further investigation with $[Ru(bpy)_3]^{2+}$, other α-diimine complexes with different one-electron redox couples, and perhaps other inert complexes capable of undergoing outer-sphere electron-transfer reactions, rather than inner-sphere reactions, which are the hallmark of ATRP.

To address the issue of poor initiation that arises, in part, from incompatibility of dicationic metal reagents with the nonpolar ATRP reaction medium, a variety of different strategies were explored. Metalloinitiator ligands and counterions were altered, and different solvents were screened. Each of these modifications is discussed in turn. Bipyridine analogues, $bpy(C_{13}H_{27})_2$, **4**, with solublizing alkyl chains were used in place of 2,2′-bipyridine to produce heteroleptic initiators with two and four reactive chloride sites **10** and **12**, respectively. With the difunctional initiator, $[Ru\{bpy(C_{13}H_{27})_2\}_2\{bpy(CH_2Cl)_2\}](PF_6)_2$, **10**, control improved for both catalyst systems in anisole solution. Initiation was more efficient with this fully soluble complex as compared to the heterogeneous analogue **5** (Table 1, compare entries 8 and 1, 9 and 2). Better correlation between calculated and experimental values observed in molecular weight vs percent monomer conversion plots lends further support to this assertion. Data obtained for the polymerization with **10** are presented in Figure 6. Polydispersities remain low (∼1.1) throughout the reaction, and only at ∼80% monomer conversion does the molecular weight begin to increase more dramatically, suggestive of radical coupling processes. Similarly, molecular weight control was better for the tetrafunctional initiator, $[Ru\{bpy(C_{13}H_{27})_2\}\{bpy(CH_2Cl)_2\}_2](PF_6)_2$, **12**. Induction periods were seen for both catalyst systems; however, the normal trend of relative rates is restored with the metalloinitiator **12** (Figure 7). That is, the $CuCl/2bpy(C_{13}H_{27})_2$ system, with a stronger metal halide bond and weaker donor ligand, favors the Cu(II) state to a lesser extent than the CuBr/HMETA catalyst, which correlates with faster rates of polymerization for CuBr/HMTETA (see Table 2, entries 10 and 12). First-order kinetics plots show some curvature, as is expected for multifunctional initiators that are prone to undergo termination by radical coupling; however, the control in these reactions improved considerably with the introduction of solubilizing $bpy(C_{13}H_{27})_2$ ligands onto the metalloinitiators.

For the homoleptic hexafunctional initiator, **7a**, it is not possible to improve solubility through derivatization of ancillary ligands. All coordination sites are occupied by ligands bearing initiator sites. Thus, other features of the metalloinitiator and ATRP reaction medium were altered in this case. In place of hexafluorophosphate, the $BAr'_4{}^-$ counterion, $B\{3,5\text{-}(CF_3)_2C_6H_3\}_4{}^-$, was introduced, which improves the solubility of cationic metal complexes in nonpolar environments.[30] Though the complex $[Ru(bpy(CH_2Cl)_2\}_3](BAr'_4)_2$, **7b**, is more soluble, kinetics experiments performed with it and the CuCl/

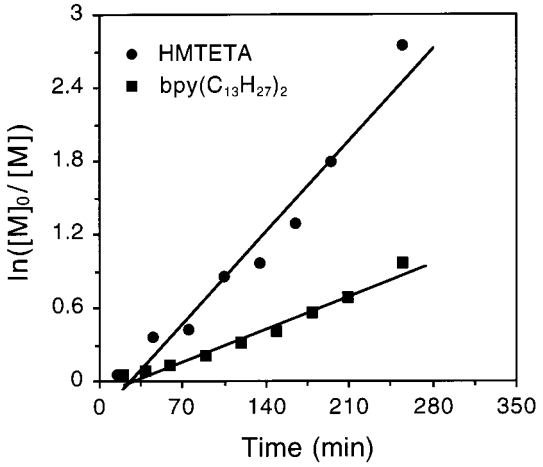

Figure 7. Comparison of first-order kinetics plots for the polymerization of styrene with the tetrafunctional metalloinitiator, $[Ru\{bpy(C_{13}H_{27})_2\}\{bpy(CH_2Cl)_2\}_2](PF_6)_2$ using the $CuCl/2bpy(C_{13}H_{27})_2$ and CuBr/HMTETA catalyst systems (Ru/Cu/L/styrene: L = $bpy(C_{13}H_{27})_2$: 1/4/8/800, L = HMTETA: 1/4/4/800; 14% anisole (v/v with styrene); 110 °C).

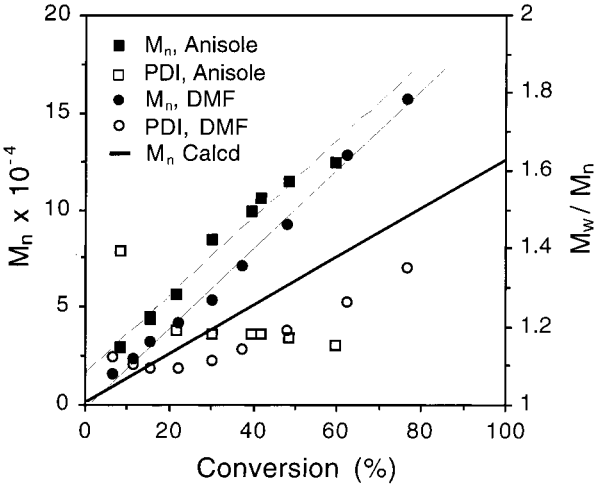

Figure 8. Comparison of M_n vs % monomer conversion plots and polydispersities for the polymerization of styrene with anisole and DMF using the hexafunctional initiator $[Ru\{bpy(CH_2Cl)_2\}_3](PF_6)_2$, **7a**, and the $CuCl/2bpy(C_{13}H_{27})_2$ catalyst system (Ru/Cu/$bpy(C_{13}H_{27})_2$/styrene = 1/6/12/1200; 14% anisole or 10% DMF (v/v with styrene); 110 °C).

$2bpy(C_{13}H_{27})_2$ catalyst displayed diminished molecular weight control relative to the di-PF_6^- salt. With BPh_4^-, counterion fragmention may generate stabilized aryl radicals that could interfere with the polymerization.[31] Perhaps a similar side reaction is occurring with **7b**. Thus, an alternative approach, namely varying the solvent, was explored.

Polymerizations run in the presence of anisole (~14% v/v) showed improved control relative to those in bulk styrene. Similarly, reactions with the hexafunctional initiator, **7a**, were improved using the more polar solvent, DMF. Others have reported that molecular weight control in styrene polymerizations increased when reactions were run in the presence of 10% DMF, which improved the solubility of the $[Cu(bpy)_2X]$ catalyst.[32] Thus, similar conditions were chosen for investigation with the DMF-soluble, hexafunctional metalloinitiator, **7a**. Number-average molecular weight vs percent monomer conversion and polydispersities for reactions of **7a** in anisole and DMF are compared in Figure 8. Although molecular weights are greater than expected on the basis of reagent loadings in both cases, the reaction run in DMF shows improved control relative to anisole reactions. Initiation is somewhat more efficient (see Table 2, entries 5 and 6), and the resulting materials show slightly better match between experimental and calculated molecular weights. At the early stages of the polymerization with DMF (<30% conversion), the PDIs are considerably lower than those for samples prepared in anisole, suggesting that DMF is a good solvent choice for the preparation of six arm stars, so long as monomer conversion is kept low. However, a steady increase in molecular weight distribution beyond this point indicated that side reactions were significant. Polydispersities were higher but more consistent for reactions run in anisole. In summary, changes in the reaction parameters that lead to better initiator solubility correlate with improved molecular weight control in the atom transfer radical polymerization of styrene.

Ruthenium Content of Polymers. By reaction design, there is to be only one $[Ru(bpy)_3]^{2+}$ moiety per macromolecule, be it a linear polymer from difunctional initiators or stars from tetra- or hexafunctional ones. Kinetics experiments have shown that polymerizations with Ru initiators are reasonably well controlled, particularly at low monomer conversions. The possibility exists, however, that the Ru(II) tris(bipyridine) complexes could act as mediators instead of initiators. Previously, Sawamoto and co-workers have exploited the redox equilibrium of Ru(II) → Ru(III) to promote the controlled ATRP of styrene.[15] However, those Ru ATRP catalysts possess open coordination sites for halide abstraction, whereas inert six-coordinate $[Ru(bpy)_3]^{2+}$ analogues do not. Even though polystyrenes described herein displayed UV/vis spectra with metal-to-ligand charge-transfer (MLCT) bands characteristic of $[Ru(bpy)_3]^{2+}$ chromophores, the complex may simply be blended with polystyrene, not covalently attached as is expected if the complex functions as an initiator. Therefore, it was necessary to determine whether the metal was indeed bound to the polymer. First, the yellow-orange color arising from Ru(II) did not disappear upon purification of the samples by filtration through alumina or precipitation of the polymers from polar (MeOH) and nonpolar (hexanes) media. Second, GPC coupled with in-line diode array UV/vis spectroscopy of eluting fractions confirmed that $[Ru(bpy)_3]^{2+}$ was associated with the polystyrene (Figure 9). These observations contrast with what was seen in control reactions involving styrene polymerization in the presence of $[Ru(bpy)_3](PF_6)_2$, a complex without initiator sites. In this case, the color washed out during polymer purification, and a white polystyrene sample resulted.

To determine whether the Ru content of polymers remained constant throughout the course of polymerization, UV/vis analysis was performed for purified samples that had been removed over the course of a polymerization from runs with metalloinitiators **5**−**7a**, **10**, and **12**. Results are collected in Table 3. Since it was difficult to obtain accurate molecular weight measurements by GPC for very low molecular weight samples isolated at the start of the reaction, and termination by radical recombination is significant at high monomer conversion, a comparison was made for different samples of moderate molecular weight. Extinction coefficients were calculated using Beer's law with concentrations that were determined using M_n values obtained by GPC. All polymers show $\pi-\pi^*$ transitions characteristic of

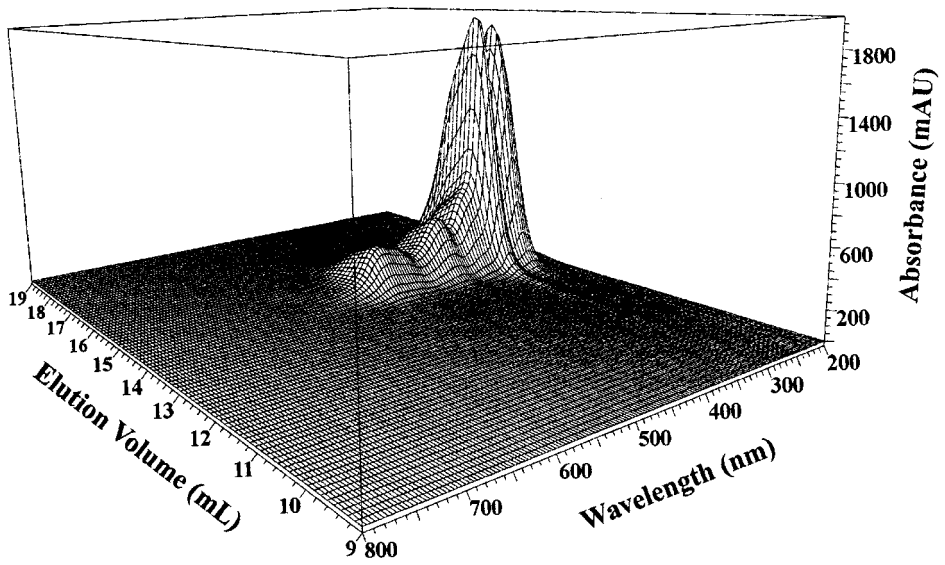

Figure 9. 3D correlation of the GPC elution volume and in-line diode array UV/vis spectra for $[Ru(bpy)_2(bpyPS_2)]^{2+}$, illustrating that the Ru initiator chromophores are associated with the polymer.

Table 3. Molecular Weight[a] and UV/Vis[b] Data for Ruthenium(II) Complexes with Polystyrene Macroligands[c]

initiator	no. arms in star	time (min)	$M_n \times 10^{-3}$	$M_w \times 10^{-3}$	M_w/M_n	λ_{max} (nm)	ϵ^e (M^{-1} cm^{-1})
5	2	120	24.6	29.8	1.21	458	19 900
5	2	210	35.2	43.6	1.23	457	19 000
5	2	330	40.0	48.2	1.20	457	21 100
6	4	40	24.3	29.6	1.22	466	20 000
6	4	120	38.5	46.6	1.21	465	18 300
6	4	180	61.1	73.9	1.21	461	19 100
7a[d]	6	30	15.1	17.0	1.12	466	19 200
7a[d]	6	90	31.5	34.4	1.09	466	19 800
7a[d]	6	150	53.3	59.3	1.11	466	19 600
10	2	90	12.1	13.1	1.08	463	20 200
10	2	195	22.1	23.7	1.07	466	19 100
10	2	315	36.6	40.7	1.11	466	18 400
12	4	40	12.5	14.3	1.15	466	18 800
12	4	90	26.1	29.7	1.14	466	20 500
12	4	150	45.9	54.9	1.20	464	19 900

[a] Molecular weight data was determined by GPC in $CHCl_3$ at 25 °C with RI and MALLS detection. [b] Concentration of $CHCl_3$ solutions was calculated using M_n as determined by GPC. [c] Polymers were prepared using CuCl/bpy($C_{13}H_{27}$)$_2$/styrene = 1:2:200 per initiating Cl site in 14% anisole (v/v vs styrene) at 110 °C. Samples were purified by passage through alumina and precipitation from THF/MeOH and CH_2Cl_2/hexanes. [d] Polymerizations were run with 10% DMF (v/v vs styrene) instead of anisole. [e] Compare to $[Ru\{bpy(C_{13}H_{27})_2\}_3](PF_6)_2$: UV/vis ($CHCl_3$) λ_{max} = 462 nm, ϵ = 18 320 M^{-1} cm^{-1}.

Table 4. Glass Transition Temperatures for Selected Ru(II)-Containing Polystyrenes and a $bpyPS_2$ Macroligand As Determined by Modulated Differential Scanning Calorimetry

polymer[a]	$M_n \times 10^{-3}$ [b]	M_w/M_n	T_g (°C)[c]
$[Ru(bpy)_2(bpyPS2)]_{2+}$	37.5	1.18	103
$[Ru(bpy)(bpyPS_2)_2]^{2+}$	41.6	1.17	98
$[Ru(bpyPS_2)_3]^{2+}$	40.2	1.25	102
$[Ru\{bpy(C_{13}H_{27})_2\}_2(bpyPS_2)]^{2+}$	35.0	1.27	103
$[Ru\{bpy(C_{13}H_{27})_2\}(bpyPS_2)_2]^{2+}$	39.5	1.17	101
$bpyPS_2$	38.3	1.20	99

[a] Polymers were prepared with the CuBr/HMTETA catalyst system. [b] Determined by GPC in $CHCl_3$ with RI and MALLS detection. [c] Reported as the middle of the change in heat capacity.

polystyrene in addition to the metal-to-ligand charge-transfer band at ~460 nm that is associated with $[Ru(bpy)_3]^{2+}$. Within the molecular weight ranges investigated, extinction coefficients vary little, and they compare favorably with the $CHCl_3$ soluble nonpolymeric complex, $[Ru\{bpy(C_{13}H_{27})_2\}_3](PF_6)_2$, **8** ($\epsilon$ = 18 320 M^{-1} cm^{-1}). In general, extinction coefficients for metallopolymers are slightly higher than those measured for the corresponding initiators. A similar trend was noted previously for polymerizations with a hexafunctional α-bromoester $Ru(bpy)_3]^{2+}$ initiator utilized in the ATRP of methyl methacrylate using $NiBr_2(PPh_3)_2$ as the catalyst.[9] It was suggested that both coupling of initiator molecules in the early stages of the polymerization and termination side reactions should lead to polymers with higher Ru content than anticipated on the basis of monomer loading. Also, side reactions in the polymerization of styrene or experimental error inherent in molecular weight determination or other measurements could account for the data that are observed. In summary, experimental evidence suggests that Ru chromophores are covalently attached to the polymer and that, on average, there is a single Ru center per polymer. Though initiation is not always optimal for reaction with metalloinitiators, so long as reactions are kept to low monomer conversion, other side reactions that are common in uncontrolled radical polymerizations are minimal.

Thermal Analysis of Bipyridine- and Ruthenium-Centered Polystyrenes. Thermal characterization by modulated differential scanning calorimetry (MDSC) was performed for $bpyPS_2$ and selected Ru-centered polymers within the molecular weight range of 35 000−41 600. In all cases, glass transitions were evident at ~100 °C. No unique trends related to differences in architecture were apparent (Table 4). In some cases, an additional thermal event resembling a glass transition was observed in certain samples; however, these features vanished after several cycles with thermal conditioning.

Conclusion

This study demonstrates that the ATRP of styrene with ligand and Ru(II) metalloinitiators is controlled, particularly if the features of the initiators are suitably modified for enhanced solubility, and the ATRP reaction

parameters are appropriately selected. The copper halide catalyst and its ligand(s) and the solvent influence these polymerizations in significant ways. Moreover, side reactions are minimized by lowering catalyst loading for CuBr/HMTETA and bulk polymerizations with CuCl/2bpy($C_{13}H_{27}$)$_2$ (but seemingly not with the latter systems in the presence of anisole or DMF) and by running reactions to low monomer conversion and not beyond. These findings are consistent with what has been observed by others for metal-free multifunctional intiators.[21−23] The synthesis of $[Ru(bpy)_3]^{2+}$ functionalized polystyrenes in this manner, with molecular weight and architectural control exceeding that obtainable by simple adsorption or "nonliving" polymerizations, lays the groundwork for further modification of these materials for use in different contexts. For example, the active halide chain ends may be exploited for the introduction of a second polymer block or for termination with various functionalities. Given the plethora of applications of luminophores in optical materials and biological contexts and the abundance of analytical techniques available for fluorescence detection, as the demand for miniaturization of devices and selectivity of agents increases, the molecular level control that is possible by controlled polymerization with stable luminescent metalloreagents is bound to become increasingly important.

Acknowledgment. We thank the National Science Foundation for PECASE and CAREER Awards, the Alfred P. Sloan Foundation for a Research Fellowship, Dupont for a Young Professor Grant, and the University of Virginia for support of this work.

Supporting Information Available: ^{1}H and ^{13}C NMR spectra for [Ru{bpy($C_{13}H_{27}$)$_2$}{bpy(CH_2Cl)$_2$}$_2$](PF_6)$_2$ (**12**). This material is available free of charge via the Internet at http://pubs.acs.org.

References and Notes

(1) (a) *Inorganic and Metal-Containing Polymeric Materials*; Sheats, J. E., Carraher, C. E., Jr., Pittman, C. U., Jr., Zeldin, M.; Currell, B., Eds.; Plenum Press: New York, 1990. (b) MacLachlan, M. J.; Ginzburg, M.; Coombs, N.; Coyle, T. W.; Raju, N. P.; Greedan, J. E.; Ozin, G. A.; Manners, I. *Science* **2000**, *287*, 1460. (c) Newkome, G. R.; He, E.; Moorefield, C. N. *Chem. Rev.* **1999**, *99*, 1689. (d) Vögtle, F.; Plevoets, M.; Nieger, M.; Azzellini, G. C.; Credi, A.; De Marchis, V.; Venturi, M.; Balzani, V. *J. Am. Chem. Soc.* **1999**, *121*, 6290.

(2) *Bioinorganic Chemistry*; Bertini, I., Gray, H. B., Lippard, S. J., Valentine, J. S., Eds.; University Science Books: Mill Valley, CA, 1994.

(3) (a) Szwarc, M.; van Beylen, M. *Ionic Polymerization and Living Polymers*; Chapman & Hall: New York, 1993. (b) Hsieh, H. L.; Quirk, R. P. *Anionic Polymerization: Principles and Practical Applications*; Marcel Dekker: New York, 1996. (c) *Cationic Polymerization: Mechanisms, Synthesis, and Applications*; Matyjaszewski, K., Ed.; Dekker: New York, 1996. (d) Kennedy, J. P.; Jacob, S. *Acc. Chem. Res.* **1998**, *31*, 835 and references therein. (e) Matyjaszewski, K.; Miller, P. J.; Fossum, E.; Nakagawa, Y. *Appl. Organomet. Chem.* **1998**, *12*, 667.

(4) For examples, see: (a) Buchmeiser, M. R. *Chem. Rev.* **2000**, *100*, 1565. (b) Mecerreyes, D.; Jérôme, R.; Dubois, P. *Novel Macromolecular Architectures Based on Aliphatic Polyesters: Relevance of the "Coordination-Insertion" Ring-Opening Polymerization*; Springer-Verlag: New York, 1999; Vol. 147. (c) Aida, T.; Inoue, S. *Acc. Chem. Res.* **1996**, *29*, 39.

(5) For a recent review see: Fraser, C. L.; Smith, A. P. *J. Polym. Sci., Part A: Chem.* **2001**, *38*, 4704.

(6) (a) McAlvin, J. E.; Scott, S. B.; Fraser, C. L. *Macromolecules* **2000**, *33*, 6953. (b) McAlvin, J. E.; Fraser, C. L. *Macromolecules* **1999**, *32*, 1341. (c) Lamba, J. J. S.; Fraser, C. L. *J. Am. Chem. Soc.* **1997**, *119*, 1801.

(7) McAlvin, J. E.; Fraser, C. L. *Macromolecules* **1999**, *32*, 6925.

(8) Collins, J. E.; Fraser, C. L. *Macromolecules* **1998**, *31*, 6715.

(9) Johnson, R. M.; Corbin, P. S.; Ng, C.; Fraser, C. L. *Macromolecules* **2000**, *33*, 7404.

(10) Corbin, P. S.; Webb, M. P.; McAlvin, J. E.; Fraser, C. L. *Biomacromolecules* **2001**, *2*, 223.

(11) Wu, X.; Fraser, C. L. *Macromolecules* **2000**, *33*, 4053.

(12) Wu, X.; Fraser, C. L. *Macromolecules* **2000**, *33*, 7785.

(13) Fraser, C. L.; Smith, A. P.; Wu, X. *J. Am. Chem. Soc.* **2000**, *122*, 9026.

(14) (a) Matyjaszewski, K. *Chem. Eur. J.* **1999**, *5*, 3095. (b) Patten, T. E.; Matyjaszewski, K. *Acc. Chem. Res.* **1999**, *32*, 895. (c) Patten, T. E.; Matyjaszewski, K. *Adv. Mater.* **1998**, *10*, 901.

(15) Sawamoto, M.; Kamigaito, M. *J. Macromol. Sci., Pure Appl. Chem.* **1997**, *A34*, 1803.

(16) (a) Fraser, C. L.; Anastasi, N. R.; Lamba, J. J. S. *J. Org. Chem.* **1997**, *62*, 9314. (b) Smith, A. P.; Lamba, J. J. S.; Fraser, C. L. *Org. Synth.*, in press.

(17) (a) Savage, S. A.; Smith, A. P.; Fraser, C. L. *J. Org. Chem.* **1998**, *63*, 10048. (b) Smith, A. P.; Savage, S. A.; Love, J. C.; Fraser, C. L. *Org. Synth.*, in press.

(18) Collins, J. E.; Lamba, J. J. S.; Love, J. C.; McAlvin, J. E.; Ng, C.; Peters, B. P.; Wu, X.; Fraser, C. L. *Inorg. Chem.* **1999**, *38*, 2020.

(19) Wang, J.-S.; Matyjaszewski, K. *J. Am. Chem. Soc.* **1995**, *117*, 5614.

(20) Xia, J.; Matyjaszewski, K. *Macromolecules* **1997**, *30*, 7697.

(21) Matyjaszewski, K.; Miller, P. J.; Pyun, J.; Kickelbick, G.; Diamanti, S. *Macromolecules* **1999**, *32*, 6526.

(22) Angot, S.; Murthy, K. S.; Taton, D.; Gnanou, Y. *Macromolecules* **2000**, *33*, 7261.

(23) Angot, S.; Murthy, K. S.; Taton, D.; Gnanou, Y. *Macromolecules* **1998**, *31*, 7218.

(24) Ueda, J.; Kamigaito, M.; Sawamoto, M. *Macromolecules* **1998**, *31*, 6762.

(25) Hovestad, N. J.; van Koten, G.; Bon, S. A. F.; Haddleton, D. M. *Macromolecules* **2000**, *33*, 4048.

(26) Keller, R. N.; Wycoff, H. D. *Inorg. Synth.* **1946**, *2*, 1.

(27) (a) Kocian, O.; Mortimer, R. J.; Beer, P. D. *Tetrahedron Lett.* **1990**, *31*, 5069. (b) Smith, A. P.; Corbin, P. S.; Fraser, C. L. *Tetrahedron Lett.* **2000**, *41*, 2787.

(28) Griggs, C. G.; Smith, D. J. *J. Chem. Soc., Perkin Trans. 1* **1982**, 3041.

(29) (a) Woodworth, B. E.; Metzner, Z.; Matyjaszewski, K. *Macromolecules* **1998**, *31*, 7999. (b) Haddleton, D. M.; Crossman, M. C.; Dana, B. H.; Duncalf, D. J.; Heming, A. M.; Kukulj, D.; Shooter, A. J. *Macromolecules* **1999**, *32*, 2110.

(30) Brookhart, M.; Grant, B.; Volpe, A. F., Jr. *Organometallics* **1992**, *11*, 3920.

(31) Tetraphenyl borate salts have been used as photoinitiators in polymerization reactions. Popielarz, R.; Sarker, A. M.; Neckers, D. C. *Macromolecules* **1998**, *31*, 951.

(32) Pascual, S.; Coutin, B.; Tardi, M.; Polton, A.; Vairon, J. P. *Macromolecules* **1999**, *32*, 1432.

MA001745S